

EXPERIMENTAL AND SIMULATION INVESTIGATION OF RFID BLIND SPOTS

C. H. Loo, A. Z. Elsherbeni, F. Yang, and D. Kajfez

Department of Electrical Engineering
The University of Mississippi
University, MS 38677, USA

Abstract—Radio-frequency identification (RFID) blind spots are the regions within the maximum operating range of the RFID system where the RFID reader fails to read the RFID tag. The existence of blind spots have troubled supply chain management and RFID system engineers because any failed or omitted reading of RFID tag would slow down the inventory tracking process. This paper studies the potential locations of blind spots as well as the effectiveness of several blind spots remedy methods such as frequency diversity, spatial diversity, polarization diversity, and antenna beam steering. Using the blind spots creation approach introduced in this paper, the locations of the blind spots can be calculated and visualized. From our simulation results, spatial diversity and polarization diversity are found to be better than all other aforementioned approaches.

1. INTRODUCTION

Ultra-high frequency (UHF) band passive RFID systems, which operate in the 860–960 MHz band, have drawn a great deal of attention. It is generally accepted that UHF RFID systems can revolutionize various commercial applications such as supply chain management and several major supply chain companies such as Wal-Mart have planned to mandate the use of UHF RFID system in their supply chains. Blind spots or dead zones often exist in the RFID system environment making the reading of RFID tag difficult. In this paper we experimentally and numerically investigate how blind spots are created and what remedies are effective in treating them.

The design of an RFID system with optimized performance is not easy for the reason of the complex RF environments. Reflective

Corresponding author: A. Z. Elsherbeni (atef@olemiss.edu).

surfaces such as walls, ceiling, and ground as well as any vicinity scatterers will generate multipath propagations of the transmitted signals. The constructive and destructive interferences of the reflected signals will create blind spots where the RFID tag is unreadable. Other factors that might incite the failure of reading of RFID tags are mainly caused by the RFID tag antenna design parameters. Those setback factors are the radiation pattern of the tag; mismatch of the tag due to the presence of metallic objects, and the mutual coupling of closely spaced tags [1–3]. Nevertheless, more blind spots would exist in more complicated environment [4].

Blind spots typically will not exist in short distance or low frequency RFID for the reason that the wavelength of the operating frequency is a lot larger than the reading distance. The failure of tag reading in short distance typically is caused by the changes of antenna design parameters. For example, the antenna impedance changes when placed close to a metallic object resulting in the impedance mismatch.

An experiment has been set up to measure the readability of RFID tag at different positions within an RFID system operating environment. Figure 1 shows the readability of an RFID tag (Alien squiggle Gen 2) measured at different positions of a vertical plane cut inside the RFID chamber at The University of Mississippi. The RFID reader used here is the ALR-9800 reader by Alien Technology. The reader transmitting antenna is circularly polarized and positioned at 4.55 feet above the ground with 1 watt output power and 6 dB gain operating at 915 MHz. The four side walls of this RFID chamber are covered by RF absorbing materials; the ceiling is opened and is assumed to have no reflection, while the ground is made of concrete to simulate the conventional RFID operating environment of a large area such as warehouse. The black pixels in the figure are the blind spots where the tag is unreadable, and the grey pixels denote a partial

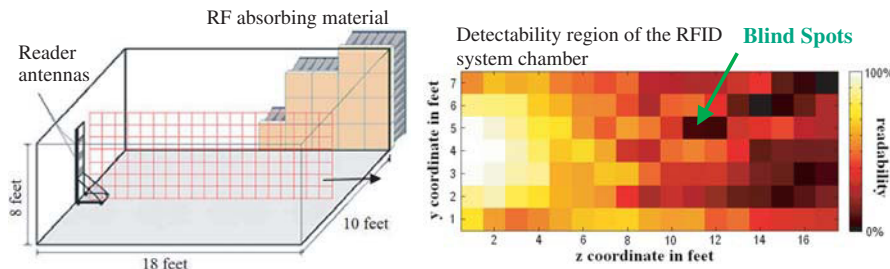


Figure 1. Measured readability of an RFID tag in the RFID chamber of university of mississippi.

readability, after several trials. The white pixels indicate maximum read rate. The results shown in this paper are for 2-dimensional cases only, the left and right side walls are always covered with RF absorbing materials. There will be more blind spots if the left and right side walls were not covered with RF absorbing materials. We have chosen not to present the 3-D cases (Faraday’s cage) for the purpose of simplifying our points. The study of the performance of RFID tag in Faraday cage can be found in the paper by Nikkari et al. [5].

The next section of this paper demonstrates the construction of blind spots in the two-dimensional central plane of the chamber, created by the reflections from the front and back walls, the ground and the ceiling of the chamber. The investigation of the effectiveness of various RFID reduction methods such as frequency diversity, spatial diversity, polarization diversity and antenna beam steering are presented in Section 3, followed by the conclusion.

2. BLIND SPOTS SIMULATION

The operation of RFID system requires the communication between the RFID reader (interrogator) and RFID tag (transponder). Figure 2 depicts the forward and backward propagations (Forward and Reverse Channels) of the RFID signals between the reader antennas and the RFID tag. The forward communication of the RFID system can be modeled by the Friis’ equation [6, p. 87]:

$$P_{tag} = P_t G_t(\theta_t, \phi_t) G_{tag} (1 - |\Gamma_t|^2) (1 - |\Gamma_{tag}|^2) \left(\frac{\lambda}{4\pi R_1}\right)^2 |\hat{\rho}_t \cdot \hat{\rho}_{tag}|^2 \quad (1)$$

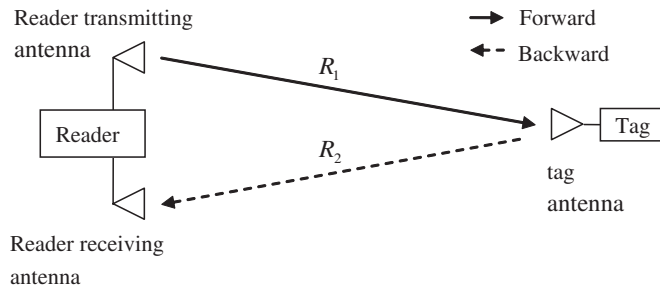


Figure 2. Forward and backward propagations of RFID system.

while the backward communication of the RFID system can be modeled by the Radar equation [6, p. 89]:

$$P_r = \sigma_{\text{tag}}(\theta_{\text{inc}}, \phi_{\text{inc}}, \theta_{\text{tag}}, \phi_{\text{tag}}) \frac{P_t G_t(\theta_t, \phi_t) G_r(\theta_r, \phi_r)}{4\pi} \left(\frac{\lambda}{4\pi R_1 R_2} \right)^2 |\hat{\rho}_r \cdot \hat{\rho}_{\text{tag}}|^2 \quad (2)$$

P_{tag} is the power received by the tag, P_t is the input power of the transmitting antenna, and G_t is the gain of the transmitting reader antenna. When the return loss of the transmitting antenna Γ_t and the cable loss are calculated to be part of the antenna gain, $P_t G_t$ is called the reader transmitted equivalent isotropic radiated power (EIRP). The gain, return loss, and radar cross section (RCS) of the tag antenna are Γ_{tag} , G_{tag} , and σ_{tag} , respectively. The power received by the receiving antenna is P_r , the gain of the receiving antenna is G_r , the distance between the transmitting antenna and the tag is R_1 , the distance between the receiving antenna and the tag is R_2 , the wavelength of the operating frequency is λ , and the polarization loss factors between the transmitting-to-tag antennas, and tag-to-receiving antennas are $|\hat{\rho}_t \cdot \hat{\rho}_{\text{tag}}|^2$ and $|\hat{\rho}_r \cdot \hat{\rho}_{\text{tag}}|^2$, respectively. Typically, the polarization loss factor for a dipole type RFID tag and circularly polarized reader antenna is 0.5. The reflective concrete ground surface is assumed to be a perfectly electrical conductive (PEC) surface. Different surface properties such as the material types, roughness, and unevenness of the surface would cause different reflected signals [7].

The radar cross section (RCS) of the tag changes between two values representing the two modulation states for backward communication. The difference of these two RCS values is called delta RCS. The larger the delta RCS value of a tag, the larger the reader-determining maximum operational distance of the system would be [8]. However, RFID maximum read range is usually limited by the tag-determining maximum operational distance that is controlled by: (1) The minimum received power required for RFID tag to operate and (2) the maximum reader EIRP allowable by the radio regulations (most countries around the world limit RFID applications to 4 watts) [9].

In the field of wireless communications, the fading of transmitted signal due to multipath propagations is known as multipath fading. There are three basic mechanisms that impact signal propagation and they are reflection, scattering, and diffraction. Reflection occurs when a signal impinges upon a surface with very large dimensions compared to the signal wavelength (λ). Scattering occurs when a signal impinges upon a surface whose dimensions are on the order of λ or less, causing the reflected energy to spread out in all directions. Diffraction is a phenomenon that accounts for the bending of signal around obstacles and the spreading out of waves past openings. In the following paragraphs, we will model the multipath propagations using

only the reflection mechanism.

The attenuation of RF energy between the transmitter and receiver in free-space is called path loss, L_{path} . The path loss taking into account of multipath fading caused by reflection at the tag location can be obtained from the power received by the tag, P_{tag} as [10]:

$$L_{\text{path}} = \frac{P_{\text{tag}}}{\text{EIRP}} \left| 1 + \sum_{n=1}^N \Gamma_n \frac{d}{d_n} e^{-j2\pi f(d_n-d)} \right|^2 \quad (3)$$

where d is the length of the direct ray path, Γ_n , is the reflection coefficient of the n -th reflecting object, d_n is the length of the n -th reflected ray path, f is the operating frequency and N is the total number of reflections. The power density at the tag location, which is the summation of the instantaneous power density at the tag location averaged over one time period, can be calculated from the following expression:

$$P_{\text{averaged}} = \text{EIRP} \times L_{\text{path}} \quad (4)$$

Figure 3 illustrates the multipath propagations and reflection of the vertical and horizontal electric components of the reader transmitted signals. Typically, the sensitivity of the reader receiving system is very high (-70 dBm to -90 dBm) while the minimum power level for the RFID tag to function is only about -10 dBm. Therefore, once a tag is activated, the backward communication signals can always be detected and thus not affecting the blind spot location [1, 11]. From Equation (1), we can calculate the power density of the transmitted signal everywhere. Most of the RFID reader antennas are circularly polarized. Circularly polarized waves can be represented by the superposition of a vertical linearly polarized wave and a horizontal linearly polarized wave with a phase difference of 90 degrees between them. The reader antennas in our lab are left-hand circularly polarized antennas. Therefore, the vertical linearly polarized component is

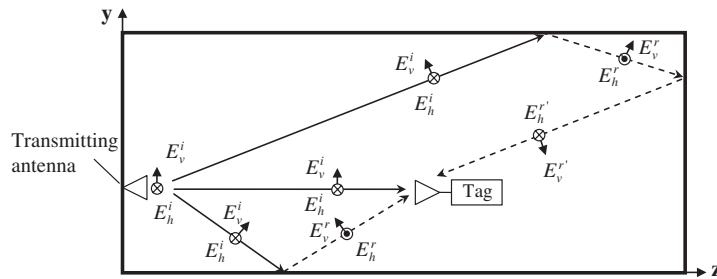


Figure 3. Multipath propagations and reflection of reader transmitted signals.

leading the horizontal linearly polarized component in the phase of 90 degrees.

The construction process of the detectable region for the horizontal electric field component is illustrated in Figure 4. The detectable region plot is based on the -11 dBm threshold value as the power required turning on the RFID tag. The radiation pattern of our reader antennas is approximated by the cosine power model as:

$$G_t = G_{t_{\max}} \times \cos^n(\theta) \quad \text{where} \quad n = \frac{\log(1/2)}{\log(\text{Beamwidth}/2)} \quad (5)$$

and $G_{t_{\max}}$ is the maximum gain of the reader antenna. The transmitting antenna is positioned at 4.55 feet above the ground and the receiving antenna is 2.91 feet above the ground. Our test reader antennas have the gain of 6 dB and beamwidth of 60 degrees. The transmitted power was rated as 1 Watt. The computed total coverage area of the detectable RFID signal in the chamber is about 93.86%

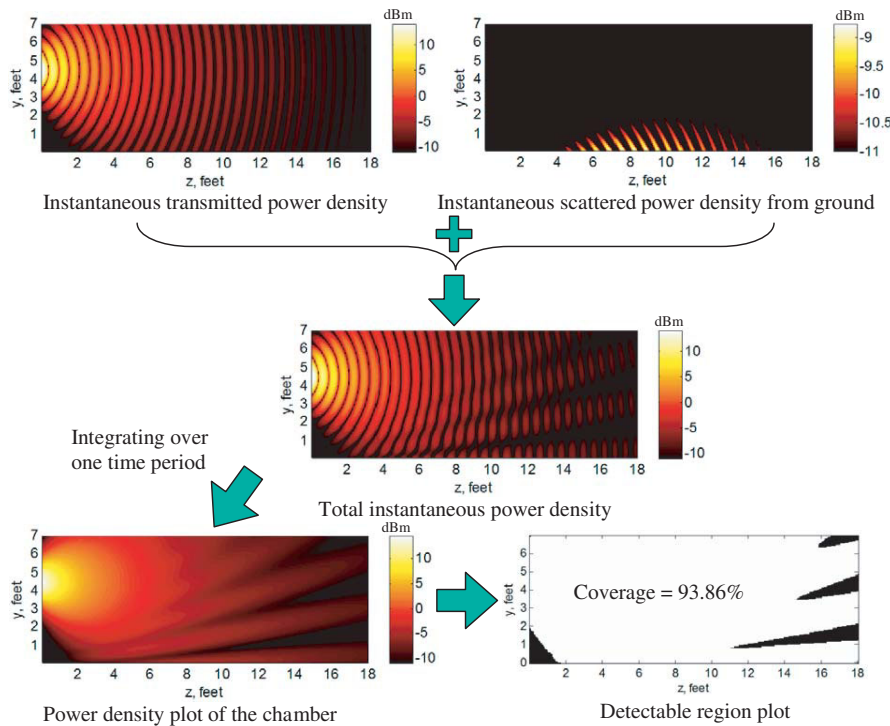


Figure 4. Detectable region plot generation process diagram for horizontal polarization.

and the rest are blind spots. In spite of the resolution differences, the simulated detectable region plot of the vertical plane cut of the chamber in Figure 4 is similar to the measured result of Figure 1 where the tag is measured with its antenna (dipole-type antenna) oriented horizontally. The detectable region plot for the vertical electric field component can be constructed in a similar way.

The plots in Figure 5 show simulations results of the chamber for horizontal linearly polarized source with (a) no reflection from anywhere, (b) chamber with reflection from ground only, (c) chamber with reflection from ceiling and ground, and (d) chamber with reflection from ceiling, ground and wall at the back of the chamber respectively. The height of the ceiling is 7.46 feet while the length is 18 feet.

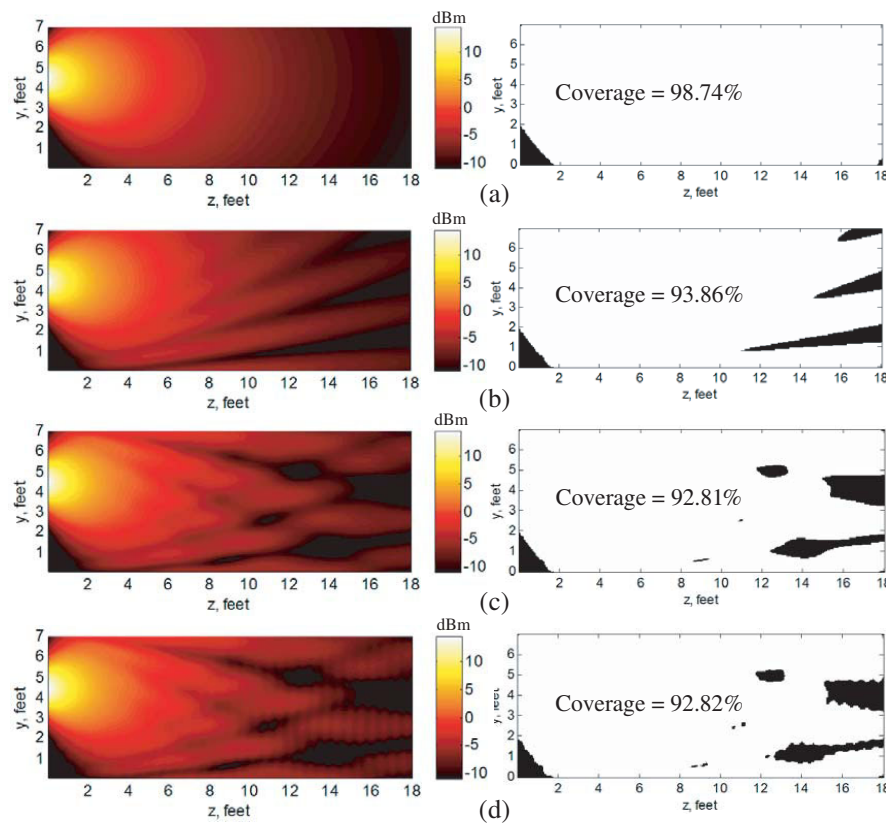


Figure 5. Power plots and the detectable region plots of the chamber for horizontal linearly polarized source with (a) no reflection, (b) ground reflection only, (c) ground and ceiling reflection only, (d) ground, ceiling and back wall reflections.

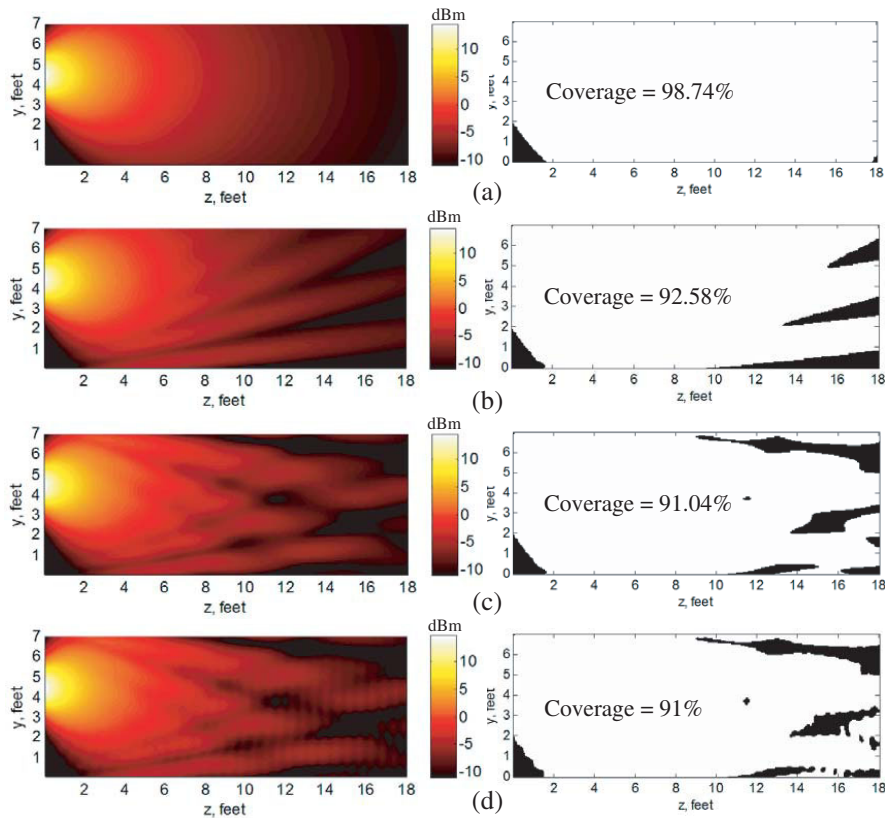


Figure 6. Power plots and the detectable region plots of the chamber for vertical linearly polarized source with (a) no reflection, (b) ground reflection only, (c) ground and ceiling reflection only, (d) ground, ceiling and back wall reflections.

of the chamber is 18 feet. We can see from the plots that additional reflective surfaces might increase or reduce blind spots. The plots in Figure 6 are simulations of the four cases of chamber for vertical linearly polarized source.

From the detectable region plots of Figures 5 and 6, we can see that the beamwidth of the transmitting antenna is not large enough to cover the entire chamber and misses a spot at the lower left corner of the chamber.

When the threshold value of turning on the tag is different from -11 dBm, the percentage coverage will have a different value. By repeating the simulations for various assumed minimum powers to turn

on the tag, one can construct diagrams shown in Figure 7. Plots of Figure 7 are the plots of the percentage coverage area versus the tag operating power for both the horizontal and the vertical polarized components respectively. In complex operating scenarios of RFID system, factors such as polarization mismatch of the tag, coupling of multiple tags, as well as nearby conductors can reduce the performance of the tag. The reduction of the tag performance can be represented by an increase in the required power level to turn on the tag.

Reflections may actually increase the maximum operating distance of an RFID system and cover larger area pervading into unwanted

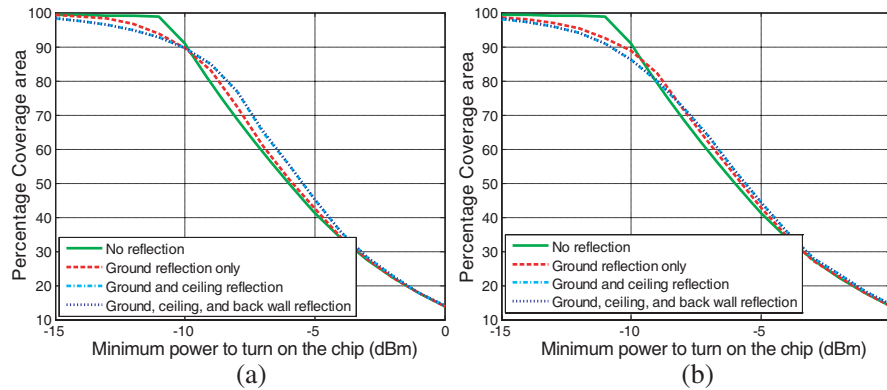


Figure 7. Percentage coverage area versus the minimum operating power of the tag plots for (a) horizontal linearly polarized, and (b) vertical linearly polarized transmitting antennas.

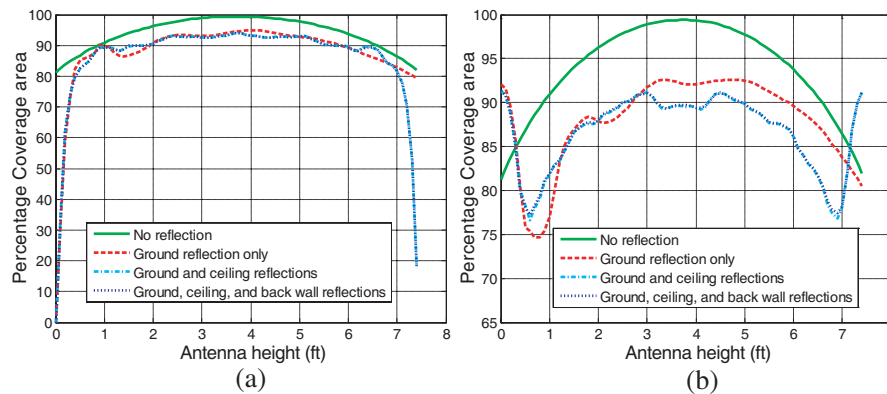


Figure 8. Percentage coverage area versus the transmitting antenna height plots for (a) horizontal linearly polarized, and (b) vertical linearly polarized transmitting antennas.

coverage area. However, blind spots will exist as long as there is a reflection.

Plotted in Figure 8 is the percentage coverage area versus the transmitting antenna position for both the horizontal and the vertical polarized components respectively. The maximum coverage happens when the transmitting antenna is positioned at the midpoint of the chamber grid height. We can also see from Figure 8(a) that the reflections will cancel the horizontal component if the transmitting antenna is positioned too close to the reflective surface.

3. BLIND SPOTS REDUCTION APPROACHES

There are several ways for mitigating multipath effects and reducing blind spots. One of the approaches is to reduce the reflection from the reflective surrounding surfaces or by maintaining the direct antenna beam illumination of reflecting surfaces to a minimum. Frequency diversity is another approach to reduce blind spots and the paper by Banerjee et al. [12] has revealed that frequency diversity is effective for long range RFID (>30 feet). Figure 9 shows the improvement of the coverage area with frequency hopping (120 MHz bandwidth 900 MHz center Frequency) comparing to single frequency operation for our chamber (ground reflection only). Nevertheless, blind spots still exist even though the entire bandwidth of global UHF RFID frequency has been used.

Spatial diversity is a good approach for mitigating blind spots. More antennas at different locations will cover more areas and reduce

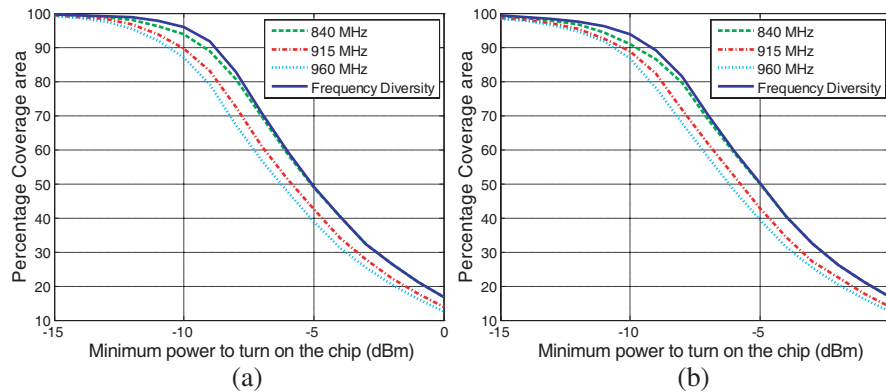


Figure 9. Frequency diversity improvement plots for (a) horizontal linearly polarized, and (b) vertical linearly polarized transmitting antennas.

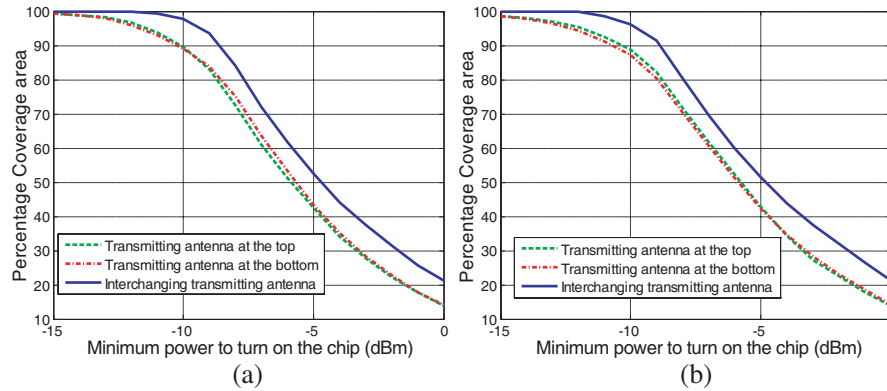


Figure 10. Spatial diversity improvement plots for (a) horizontal linearly polarized, and (b) vertical linearly polarized transmitting antennas.

blind spots. The greater distance between the transmitting antennas, the larger areas they will cover. Most RFID readers have the capability of taking multiple reading while switching the role of the connected antennas to be either transmitting antenna or receiving antenna. For example, in the first read, antenna A is transmitting and antenna B is receiving, in the second read, antenna B is transmitting and antenna A is receiving. Figure 10 illustrates the improvement of signal coverage by interchanging the roles of the transmitting and receiving antennas positioned 1.64 feet apart at 915 MHz operating frequency. If multiple readers are employed, the reader-to-reader interference between the vicinity reader antennas would cause the read range of the individual reader antenna to be reduced [13]. In conclusion, spatial diversity seems to be quite efficient in eliminating blind spots.

A reader antenna transmitting a vertical linearly polarized signal will not be able to read a horizontally polarized receiving antenna (horizontally oriented dipole tag antenna). Similarly, a horizontally polarized reader antenna will not be able to read a vertically polarized tag antenna. Polarization diversity is the use of more than one polarization in the communication between the transmitter and receiver. Most of the RFID reader antennas are circularly polarized and most of the RFID tags have dipole-type linearly polarized antennas. This can be considered partially polarization diversified because the reader antenna transmits both vertically and horizontally polarized signals. However, a dual linearly polarized tag is required to read both of the vertically and the horizontally polarized signals at its receiving position. A dual polarized tag consists of a multiple

ports dual polarized tag antenna connected to a multiple ports RFID chip. The signals from those ports can be combined to make it less sensitive to tag orientation [14]. A dual polarized reader antenna can consecutively operate in two polarizations. For example, the reader transmits vertically polarized signal in its first reading and then switch to horizontally polarized signal in the next reading [15]. Shown in Figure 11 is the improvement of signal coverage by a dual polarized tag antenna comparing to a vertically polarized tag and a horizontally polarized tag. The blind spots locations of one polarization source seldom overlap the blind spots locations of another polarization source. As the result, this remedy approach is efficient and is very suitable for portable RFID reader with just a single antenna for transmitting and receiving.

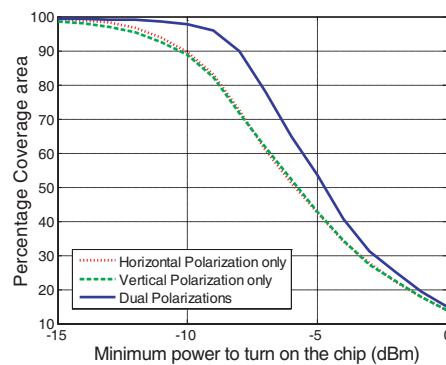


Figure 11. Dual polarizations improvement plot.

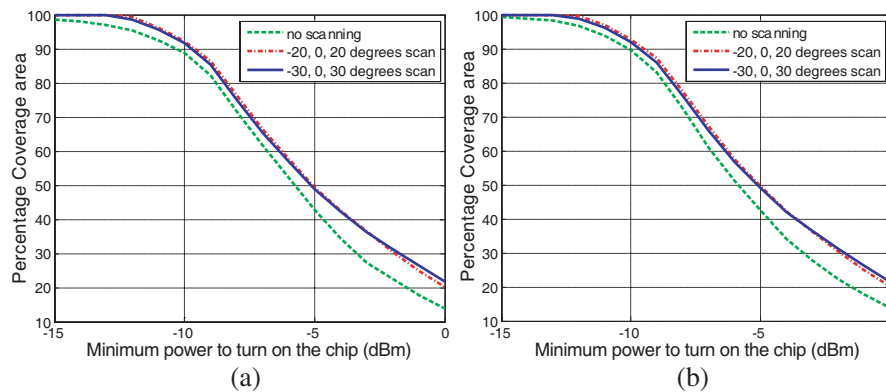


Figure 12. Directional scanning transmitting antenna coverage plots for (a) horizontal linearly polarized, and (b) vertical linearly polarized transmitting antennas.

Changing the transmitting antennas orientation will also improve the coverage area and therefore an antenna with direction scanning ability will be able to cover larger detectable area. The scanning of antennas can be either electrical or mechanical. The plots of Figure 12 show the results of a simulated mechanical direction scanning transmitting antenna. The scanning angles of the simulations are 0, 20 and 30 degrees respectively each making 3 readings per scan. Better coverage improvement can be obtained from larger total scan angle or smaller scanning angle. For the reason that directional steer-able antenna requires additional circuitry or mechanical part. Direction scanning might be too costly for the benefit it offers.

4. CONCLUSION

Blind spots will exist in large area where the RFID operating distance is greater than the wavelength of the operating frequency. For complete and successful operation of RFID systems in a large area, blind spots are to be eliminated. This paper presents multiple approaches to achieve this goal. Because of the limited band of the allowed operating frequencies, the frequency diversity approach does not provide a suitable solution for effectively eliminating the blind spots. Spatial diversity with multiple reader antennas and polarization diversity with dual polarized antennas are both found to be effective ways for significantly reducing blind spots. A single reader antenna with directional scanning ability will also reduce blind spots but may be too pricey due to the required additional hardware components. Combination of the aforementioned approaches could also be used for even better reduction of blind spots.

REFERENCES

1. Li, H., H. Lin, and H. Wu, "Effect of antenna mutual coupling on the UHF passive RFID tag detection," *2008 IEEE AP-S International Symposium and USNC/URSI National Radio Science Meeting*, Jul. 2008.
2. Kuo, S.-K., S.-L. Chen, and C.-T. Lin, "An accurate method for impedance measurement of RFID tag antenna," *Progress In Electromagnetics Research*, PIER 83, 93–106, 2008.
3. Fan, Z.-G., S. Qiao, J.-T. Huangfu, and L.-X. Ran, "A miniaturized printed dipole antenna with V-shaped ground for 2.45 GHz RFID readers," *Progress In Electromagnetics Research*, PIER 71, 149–158, 2007.

4. Seow, C.-K. and S.-Y. Tan, "Localization of omni-directional mobile device in multipath environments," *Progress In Electromagnetics Research*, PIER 85, 323–348, 2008.
5. Nikkari, M., T. Björninen, L. Sydänheimo, L. Ukkonen, A. Z. Elsherbeni, F. Yang, and M. Kivikoski, "Performance of a passive UHF RFID tag in reflective environment," *2008 IEEE AP-S International Symposium and USNC/URSI National Radio Science Meeting*, Jul. 2008.
6. Balanis, C. A., *Antenna Theory: Analysis and Design*, 2nd edition, John Wiley and Sons, 1996.
7. Popov, A.-V. and V.-V. Kopeikin, "Electromagnetic pulse propagation over nonuniform earth surface: Numerical simulation," *Progress In Electromagnetics Research B*, Vol. 6, 37–64, 2008.
8. Fan, Z.-G., S. Qiao, J.-T. Huangfu, and L.-X. Ran, "Signal descriptions and formulations for long range UHF RFID readers," *Progress In Electromagnetics Research*, PIER 71, 109–127, 2007.
9. Loo, C.-H., K. Elmahgoub, F. Yang, A. Elsherbeni, D. Kajfez, A. Kishk, and T. Elsherbeni, "Chip impedance matching for UHF RFID tag antenna design," *Progress In Electromagnetics Research*, PIER 81, 359–370, 2008.
10. Bianchi, C. H. and K. Sivaprasad, "A channel model for multipath interference on terrestrial line-of-sight digital radio," *IEEE Transactions on Antennas and Propagation*, Vol. 46, No. 6, 891–901, Jun. 1998.
11. Li, H.-J., T.-Y. Liu, and J.-L. Leou, "Antenna measurements in the presence of multipath waves," *Progress In Electromagnetics Research*, PIER 30, 157–178, 2001.
12. Banerjee, S.-R., R. Jesme, and R.-A. Sainati, "Investigation of spatial and frequency diversity for long range UHF RFID," *2008 IEEE AP-S International Symposium and USNC/URSI National Radio Science Meeting*, Jul. 2008.
13. Kim, D.-Y. and J.-G. Yook, "Interference analysis of UHF RFID systems," *Progress In Electromagnetics Research B*, Vol. 4, 115–126, 2008.
14. Nikitin, P. V. and K. V. S. Rao, "Performance of RFID tags with multiple RF ports," *IEEE Antennas and Propagation Symposium*, Honolulu, HI, Jun. 2007.
15. Kim, J.-S., K.-H. Shin, S.-M. Park, W.-K. Choi, and N.-S. Seong, "Polarization and space diversity antenna using inverted-F antennas for RFID reader applications," *IEEE AWP Letters*, Vol. 5, No. 1, 265–268, Dec. 2006.

Copyright of *Journal of Electromagnetic Waves & Applications* is the property of VSP International Science Publishers and its content may not be copied or emailed to multiple sites or posted to a listserv without the copyright holder's express written permission. However, users may print, download, or email articles for individual use.